doi:10.1093/brain/awaa025 BRAIN 2020: 143; 1027–1038 | 1027

BRAIN
A JOURNAL OF NEUROLOGY

Two distinct neuroanatomical subtypes of schizophrenia revealed using machine learning

Ganesh B. Chand,[1,2,*] Dominic B. Dwyer,[3,*] Guray Erus,[1,2] Aristeidis Sotiras,[1,2,4] Erdem Varol,[1,2,5] Dhivya Srinivasan,[1,2] Jimit Doshi,[1,2] Raymond Pomponio,[1,2] Alessandro Pigoni,[3,6] Paola Dazzan,[7] Rene S. Kahn,[8] Hugo G. Schnack,[9] Marcus V. Zanetti,[10,11] Eva Meisenzahl,[12] Geraldo F. Busatto,[10] Benedicto Crespo-Facorro,[13,14] Christos Pantelis,[15] Stephen J. Wood,[16,17,18] Chuanjun Zhuo,[19,20] Russell T. Shinohara,[2,21] Haochang Shou,[2,21] Yong Fan,[1,2] Ruben C. Gur,[1,22] Raquel E. Gur,[1,22] Theodore D. Satterthwaite,[2,22] Nikolaos Koutsouleris,[3] Daniel H. Wolf[2,22,#] and Christos Davatzikos[1,2,#]

*,#These authors contributed equally to this work.

Neurobiological heterogeneity in schizophrenia is poorly understood and confounds current analyses. We investigated neuroanatomical subtypes in a multi-institutional multi-ethnic cohort, using novel semi-supervised machine learning methods designed to discover patterns associated with disease rather than normal anatomical variation. Structural MRI and clinical measures in established schizophrenia ($n = 307$) and healthy controls ($n = 364$) were analysed across three sites of PHENOM (Psychosis Heterogeneity Evaluated via Dimensional Neuroimaging) consortium. Regional volumetric measures of grey matter, white matter, and CSF were used to identify distinct and reproducible neuroanatomical subtypes of schizophrenia. Two distinct neuroanatomical subtypes were found. Subtype 1 showed widespread lower grey matter volumes, most prominent in thalamus, nucleus accumbens, medial temporal, medial prefrontal/frontal and insular cortices. Subtype 2 showed increased volume in the basal ganglia and internal capsule, and otherwise normal brain volumes. Grey matter volume correlated negatively with illness duration in Subtype 1 ($r = –0.201$, $P = 0.016$) but not in Subtype 2 ($r = –0.045$, $P = 0.652$), potentially indicating different underlying neuropathological processes. The subtypes did not differ in age ($t = –1.603$, df = 305, $P = 0.109$), sex (chi-square = 0.013, df = 1, $P = 0.910$), illness duration ($t = –0.167$, df = 277, $P = 0.868$), antipsychotic dose ($t = –0.439$, df = 210, $P = 0.521$), age of illness onset ($t = –1.355$, df = 277, $P = 0.177$), positive symptoms ($t = 0.249$, df = 289, $P = 0.803$), negative symptoms ($t = 0.151$, df = 289, $P = 0.879$), or antipsychotic type (chi-square = 6.670, df = 3, $P = 0.083$). Subtype 1 had lower educational attainment than Subtype 2 (chi-square = 6.389, df = 2, $P = 0.041$). In conclusion, we discovered two distinct and highly reproducible neuroanatomical subtypes. Subtype 1 displayed widespread volume reduction correlating with illness duration, and worse premorbid functioning. Subtype 2 had normal and stable anatomy, except for larger basal ganglia and internal capsule, not explained by antipsychotic dose. These subtypes challenge the notion that brain volume loss is a general feature of schizophrenia and suggest differential aetiologies. They can facilitate strategies for clinical trial enrichment and stratification, and precision diagnostics.

1 Department of Radiology, Perelman School of Medicine, University of Pennsylvania, Philadelphia, USA
2 Center for Biomedical Image Computing and Analytics, Perelman School of Medicine, University of Pennsylvania, Philadelphia, USA
3 Department of Psychiatry and Psychotherapy, Ludwig-Maximilian University, Munich, Germany
4 Department of Radiology, School of Medicine, Washington University in St. Louis, St. Louis, USA
5 Department of Statistics, Zuckerman Institute, Columbia University, New York, USA
6 Department of Neurosciences and Mental Health, University of Milan, Milan, Italy
7 Institute of Psychiatry, King's College London, London, UK

Received September 27, 2019. Revised November 19, 2019. Accepted December 16, 2019. Advance access publication February 27, 2020

8 Department of Psychiatry, Icahn School of Medicine at Mount Sinai, New York, USA
9 Department of Psychiatry, University Medical Center Utrecht, Utrecht, The Netherlands
10 Institute of Psychiatry, Faculty of Medicine, University of São Paulo, São Paulo, Brazil
11 Hospital Sírio-Libanês, São Paulo, Brazil
12 LVR-Klinikum Düsseldorf, Kliniken der Heinrich-Heine-Universität, Düsseldorf, Germany
13 University of Cantabria; IDIVAL-CIBERSAM, Cantabria, Spain
14 Department of Psychiatry, School of Medicine, University Hospital Virgen del Rocio, University of Sevilla, Spain
15 Melbourne Neuropsychiatry Centre, Department of Psychiatry, University of Melbourne and Melbourne Health, Carlton South, Australia
16 Orygen, National Centre of Excellence for Youth Mental Health, Melbourne, Australia
17 Centre for Youth Mental Health, University of Melbourne, Melbourne, Australia
18 School of Psychology, University of Birmingham, Edgbaston, UK
19 Department of Psychiatric-Neuroimaging-Genetics and Co-morbidity Laboratory (PNGC-Lab), Nankai University Affiliated Tianjin Anding Hospital, Tianjin Medical University, Tianjin, China
20 Department of Psychiatry, Tianjin Medical University, Tianjin, China
21 Department of Biostatistics, Epidemiology, and Informatics, Perelman School of Medicine, University of Pennsylvania, Philadelphia, USA
22 Department of Psychiatry, Perelman School of Medicine, University of Pennsylvania, Philadelphia, USA

Correspondence to: Ganesh B Chand, PhD
3700 Hamilton Walk, Philadelphia, PA 19104, USA
E-mail: ganesh.chand@pennmedicine.upenn.edu

Correspondence may also be addressed to: Christos Davatzikos, PhD
E-mail: christos.davatzikos@pennmedicine.upenn.edu

Keywords: schizophrenia; structural MRI; neuroanatomical heterogeneity; semi-supervised machine learning; voxel-wise analysis

Abbreviations: ARI = adjusted Rand Index; HYDRA = heterogeneity through discriminative analysis

Introduction

The diagnosis of schizophrenia encompasses individuals with well-known variability in clinical presentation (Derks *et al.*, 2012), illness course (Carpenter and Kirkpatrick, 1988), treatment response (Palaniyappan *et al.*, 2013), functional outcome (Fett *et al.*, 2011), and biomarker expression (Arnedo *et al.*, 2015; Clementz *et al.*, 2016). It has long been appreciated that such heterogeneity undermines the precision of clinical treatment guidelines and obscures research findings (Insel and Cuthbert, 2015). Still, research attempting to dissect such heterogeneity using symptom subtyping (Koutsouleris *et al.*, 2008; Voineskos *et al.*, 2013; Nenadic *et al.*, 2015) has had little impact on research and practice; indeed, diagnostic systems have removed most symptom-based schizophrenia subtypes from classification schemes (e.g. DSM-V). Direct stratification of biological heterogeneity may have greater impact by objectively identifying subtypes (Varol *et al.*, 2017) using structural MRI (Abi-Dargham and Horga, 2016).

Prior neuroimaging research has primarily used binary case-control designs to investigate neuroanatomical abnormalities in schizophrenia. These analyses predominantly show widespread, subtle brain volume decreases (Koutsouleris *et al.*, 2008; Gupta *et al.*, 2015; Clementz *et al.*, 2016). In addition to distributed deficits, increased basal ganglia volume has been reported in large samples, including the ENIGMA and COCORO consortia (Okada *et al.*, 2016; van Erp *et al.*, 2016), and our own group (Rozycki *et al.*, 2018). It is unclear whether both of these alterations exist in the same individuals or whether these effects are representative of different underlying subtypes. Studies defining schizophrenia subtypes based on symptoms have indicated that individuals with more negative symptoms exhibit more widespread cortical volume decreases compared to other subtypes (Koutsouleris *et al.*, 2008; Voineskos *et al.*, 2013; Nenadic *et al.*, 2015; Zhang *et al.*, 2015*a*), but the brain signatures are overlapping and they do not clarify the volumetric increases and decreases found in large studies.

Objectively defining biological subtypes based on neuroanatomical data is important for further progress. Prior 'biotype' research has examined other phenotypes, including genes (Arnedo *et al.*, 2015), functional MRI (Du *et al.*, 2015), or combinations of electrophysiology and cognition (Clementz *et al.*, 2016). Only two prior studies have sought to directly parse neuroanatomical heterogeneity in schizophrenia (Honnorat *et al.*, 2017; Dwyer *et al.*, 2018). However, those investigations were limited by insufficient sample diversity and small sample size, which hindered rigorous reproducibility analyses of subtypes such as split-sample reproducibility, leave-one-site-out validation, sex-specific evaluation, and sample restriction within 45 years of age to minimize ageing effects. Although one of the studies (Dwyer *et al.*, 2018) benefitted from external validation set, the method used in that study was not specifically designed to identify the patient subtypes based on their variation from healthy controls to capture the disease effects better. Taken together, these factors might have led to less

reproducible subtypes and overlapping subtype profiles that impeded clear interpretation.

Progress in delineating schizophrenia brain subtypes requires increased sample sizes, increased sample heterogeneity, and methodological advances that generalize across disparate sites and ethnicities. To respond to this challenge, we established a consortium spanning three continents called PHENOM ('Psychosis Heterogeneity Evaluated via Dimensional Neuroimaging'). We then sought to identify neuroanatomical subtypes by applying a recently developed semi-supervised machine learning method termed HYDRA (heterogeneity through discriminative analysis) (Varol *et al.*, 2017). HYDRA is fundamentally different from previous clustering methods (Fair *et al.*, 2012; Arnedo *et al.*, 2015; Du *et al.*, 2015; Clementz *et al.*, 2016) because it specifically seeks to cluster illness effects by modelling differences from healthy controls rather than clustering patients directly. This approach helps identify true disease subtypes by limiting the influence of confounding variations introduced by age, sex, scanner, ethnicity, and other factors. This is the case because all these confounding variations are already present in the control group, while only differences between patients and controls, presumably due to pathological processes, are clustered. We hypothesized that this method would objectively reveal distinct neuroanatomical subtypes that were previously obscured in typical case-control designs, and that were not explained by illness duration or antipsychotic dose.

Materials and methods

Study sample and image acquisition

This study investigated a PHENOM subsample collected from three sites (Satterthwaite *et al.*, 2010; Wolf *et al.*, 2014; Zhang *et al.*, 2015*a*; Zhu *et al.*, 2016; Zhuo *et al.*, 2016) (US, German and Chinese cohorts; see Supplementary material). We intentionally selected samples from diverse imaging protocols, including 1.5 T data from Germany, because this provides an opportunity to generalize our subtypes across a wide range of currently available MRI protocols. To ensure that the subtypes were not site/protocol biased, we further validated the subtypes by examining leave-one-site-out reproducibility. Images were shared by respective investigators and analysed at the Center for Biomedical Image Computing and Analytics of the University of Pennsylvania. From an international cohort of 941 schizophrenia patients and controls, we restricted our analyses to subjects of age 45 years or less to reduce ageing effects. Demographics for the resultant sample (307 schizophrenia patients and 364 healthy controls) are presented in Table 1, which reflects the diversity of the consortium cohort and MRI scans.

Image preprocessing

Individuals' T_1 images were checked for quality (Supplementary material) and a state-of-the-art multi-atlas segmentation (Doshi *et al.*, 2016) was used to obtain anatomical regions of interest consisting of grey matter, white matter and CSF. Regional

Table 1 Sample demographics

	Harmonized (*n* = 671)		Site 1 (Penn) (*n* = 227)		Site 2 (Munich) (*n* = 302)		Site 3 (Tianjin) (*n* = 142)	
	Controls	Patients	Controls	Patients	Controls	Patients	Controls	Patients
n	364	307	131	96	157	145	76	66
Age, mean years (SD)	29.5 (7.0)	30.9 (7.3)	29.5 (6.8)	31.8 (7.5)	30.6 (6.9)	29.7 (7.1)	32.2 (6.7)	29.9 (7.4)
Female, *n* (%)	161 (44.2)	108 (35.2)	77 (58.8)	44 (45.8)	46 (29.3)	33 (22.8)	38 (50.0)	31 (46.9)
CPZ, mean (min–max), *n*	NA	418.6 (0.0–1850.0), 212	NA	431.6 (100.0–1400.0), 44	NA	388.3 (10.0–1850.0), 115	NA	473.5 (0.0–1775.0), 53
Duration of illness, mean years (min–max), *n*	NA	7.1 (0.0–29.6), 279	NA	11.7 (0.6–29.6), 84	NA	3.8 (0.0–26.1), 142	NA	8.8 (0.0–25.0), 53
Age of illness onset, mean years (min–max), *n*	NA	23.8 (10.0–43.0), 279	NA	20.5 (10.0–36.0), 84	NA	25.7 (15.2–42.3), 142	NA	24.2 (15.0–43.0), 53
Clinical symptom score, *n* (%), type	NA	291 (94.8), various	NA	93 (96.9), SANS/SAPS	NA	145 (100.0), PANSS	NA	53 (80.3), PANSS
Antipsychotic generation, *n* (%)	NA	207 (67.4)	NA	84 (87.5)	NA	123 (84.8)	NA	0 (0.0)
MRI protocol	Various		MPRAGE		MPRAGE		BRAVO	
Magnetic field strength	Various		3 T		1.5 T		3 T	
Acquisition location	Various		University of Pennsylvania, Philadelphia, PA, USA		Ludwig-Maximilian University, Munich, Germany		Tianjin Anning Hospital, Tianjin, China	

BRAVO = Brain Volume sequence; MPRAGE = magnetization prepared rapid acquisition gradient; NA = not applicable; PANSS = Positive and Negative Symptoms Scale; SANS = Scale for the Assessment of Negative Symptoms; SAPS = Scale for the Assessment of Positive Symptoms.

volumetric maps (Davatzikos *et al.*, 2001), which provide highly localized voxel-wise patterns compared to region of interest-based maps and have been used successfully to visualize group differences (Zhang *et al.*, 2015*a*; Dong *et al.*, 2017), were generated for grey matter, white matter and CSF.

Inter-site image harmonization and correction of covariates

Site-specific effects in the region of interest volumes were estimated using a linear model from a subsample of healthy control subjects, which contained an equal proportion of males and females from each site [mean age (standard deviation, SD) years: 29.97 (7.13) in Penn, 29.39 (6.17) in Munich, 29.04 (7.54) in Tianjin; $P > 0.46$], and were removed from all (including patient) data. After calibration for site effects, region of interest volumes were adjusted for age and sex; thus, all clustering results reported here are independent of site, age and sex. This pooled healthy control-based harmonization and covariate adjustment procedure was also applied to voxel-wise volumetric maps.

Subtyping schizophrenia with HYDRA

We applied HYDRA (Varol *et al.*, 2017) to region of interest volume measures to identify subtypes. HYDRA compares patients and controls to identify the subtypes within the patients. Unlike fully supervised learning methods such as support vector machines and random forests, which cannot distinguish between the subtypes of patients, HYDRA performs classification and clustering simultaneously. Classification is performed through the separation of healthy controls from patients by the polytope formed by linear maximum-margin classifiers. Subtyping is carried out by clustering patients through their association with different faces of the polytope known as hyperplanes. In contrast to unsupervised clustering algorithms such as k-means, which cluster patients based on their similarities, and are vulnerable to confounding inter-individual variations irrelevant to disease (e.g. age or sex), HYDRA effectively clusters patients based on their differences from controls. This method is flexible in terms of evaluating higher number of subtypes by varying the number of hyperplanes. HYDRA is described in the Supplementary material.

Reproducibility analysis of schizophrenia subtypes

Subtype reproducibility was extensively analysed using (i) permutation tests (Nichols and Homes, 2001) to test statistical significance; (ii) split-sample methods (Ben-Hur *et al.*, 2002; Lange *et al.*, 2004) to evaluate whether the subtypes in each half exhibit similar profiles; and (iii) leave-one-site-out validation (Arlot and Celisse, 2010) to examine whether the subtypes found using this method are consistent with the solution obtained from taking all the sites together (see details in the Supplementary material).

Voxel-wise analysis

We conducted voxel-wise volumetric analyses using regionally linear multivariate discriminative statistical mapping (MIDAS) (Varol *et al.*, 2018) to explore the neuroanatomical alterations of subtypes. MIDAS leverages the power of regional discriminant analysis and achieves relatively higher sensitivity and specificity in detecting group differences compared to other information-mapping methods (e.g. Searchlight). MIDAS is detailed in the Supplementary material.

Clinical examination of schizophrenia subtypes

Within each subtype, the relationship between total grey matter volume and illness duration was assessed using Pearson's correlation. Two-sample *t*-tests were used to assess differences between subtypes in age, illness duration, chlorpromazine-equivalent dose (mg) per day (CPZ mg eq/day), age of illness onset, positive symptoms, and negative symptoms (see details in the Supplementary material). Sex, education (ordinal scale), and antipsychotic type (first versus second-generation) were compared using the chi-square test.

Data availability

The subtype memberships that support the findings of this study are available upon reasonable request. The regions of interest volumes for Site 1 (Penn, USA) and Site 3 (Tianjin, China) are also available. The regions of interest volumes for Site 2 (Munich, Germany) will be shared following the European regulations.

Results

HYDRA reveals two highly reproducible subtypes

In the standard case-control comparison, both volume decreases and increases are present (Supplementary Fig. 1), but it is not clear whether some or all of these effects are contributed by the entire population or by certain subgroups of patients. HYDRA effectively addresses this issue, as presented below. We applied HYDRA to the volumes of anatomical regions of interest (Supplementary Table 1) to identify subtypes. We evaluated the consistency of clustering assignment over multiple resolutions (two to eight clusters) using the adjusted Rand Index (ARI) (Hubert and Arabie, 1985), which is relatively insensitive to the number of clusters (K). The ARI at $K = 1$ is not meaningful as it corresponds to the trivial solution of assigning all patients to the same group by definition. However, if the sample is best understood as homogenous (optimal $K = 1$) then low ARIs should be found for other values of K. The maximum reproducibility was found at $K = 2$ solution, with ARI = 0.616 (Supplementary Fig. 2). The ARIs for $K = 3$ to 8 were ~0.4 and were lower than the ARI at $K = 2$. The distribution of schizophrenia patients across K's and sites is presented in

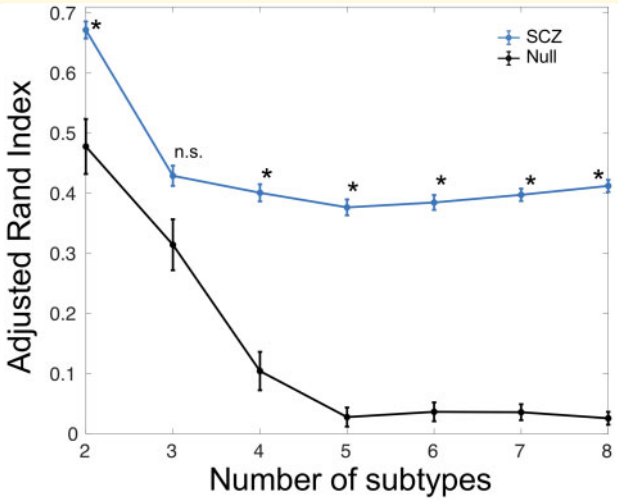

Figure 1 Statistical significance of ARI obtained for different subtypes (K) via comparison with the null distribution obtained from random permutations. *FDR-corrected $P < 10^{-3}$ for comparison between Null and schizophrenia (SCZ). n.s. = not significant.

the Supplementary Table 2. At K = 2, there are larger number of patients assigned to Subtype 1 in each site. To determine statistical significance of clusters, we compared the ARI at each cluster to a null distribution that was generated using permutation tests. The ARI at K = 2 was higher than from null distribution ($P_{FDR} < 10^{-3}$) (Fig. 1), but not at K = 3. The ARIs for K = 4 to 8 were also higher than those from null distribution; however, clustering into K = 3 or more introduced sex, age or site differences among subtypes (Supplementary Tables 2–9). The superior reproducibility of K = 2 solution was also seen in the split-half comparisons compared to other clustering solutions (Supplementary Fig. 3). The voxel-wise volumetric patterns were also reproducible between Split 1 and Split 2 at K = 2 but not for other K's (Supplementary Figs 4 and 5). Furthermore, the reproducibility analyses of the subtypes were carried out using the leave-one-site-out approach (Supplementary Fig. 6). The predicted Subtype 1 and Subtype 2 assignments from all three sites using leave-one-site-out were compared with the original assignments obtained by taking all the sites together (Supplementary Table 2: K = 2). The percentage overlap of patients that were assigned to the same subtype was 86.72% (83.33% in Site 1, 86.21% in Site 2 and 90.63% in Site 3). The two subtypes were also reproducible across the sites (Supplementary Fig. 7). Given these convergent results, subsequent analyses focused on the two highly reproducible subtypes.

Subtypes exhibit divergent neuroanatomical deficits

Subtypes showed marked differences in their voxel-wise patterns of neuroanatomical deficits (Fig. 2). Subtype 1 showed a distributed pattern of grey matter deficits compared to healthy controls (Fig. 2A) and Subtype 2 (Supplementary Fig. 8). Compared to healthy controls, Subtype 1 abnormalities were most prominent in the thalamus, nucleus accumbens, medial temporal, medial prefrontal, and insular cortices. Additionally, Subtype 1 showed widespread reductions in white matter volumes (Fig. 2C). In contrast, Subtype 2 had normal brain anatomy, except for exhibiting larger grey matter volumes of the basal ganglia (pallidum, putamen and parts of caudate) (Fig. 2B). White matter volume was also relatively larger in deep structures, especially internal capsule, of Subtype 2, when compared with healthy controls (Fig. 2D). Compared to healthy controls, both subtypes had mildly elevated CSF, mainly in third ventricle and frontal inter-hemispheric fissure (Supplementary Fig. 9).

Subtype profiles show robust reproducibility in the leave-one-site-out validation

The predicted subtypes using the leave-one-site-out method showed excellent reproducibility (Fig. 3) with the results obtained by taking all the sites together (Fig. 2). Consistent with the above results, Subtype 1 abnormalities were widespread and most noticeable in the thalamus, nucleus accumbens, medial temporal, medial prefrontal, and insular cortices (Fig. 3A) and Subtype 2 had larger volume in the basal ganglia (Fig. 3B). Subtype 1 also showed a distributed pattern of grey matter deficits compared to Subtype 2 (Supplementary Fig. 10), which was consistent with the above results (Supplementary Fig. 8).

Sensitivity analyses provide convergent results

Next, we conducted extensive sensitivity analyses to ensure the above results were not driven by sample size, sex

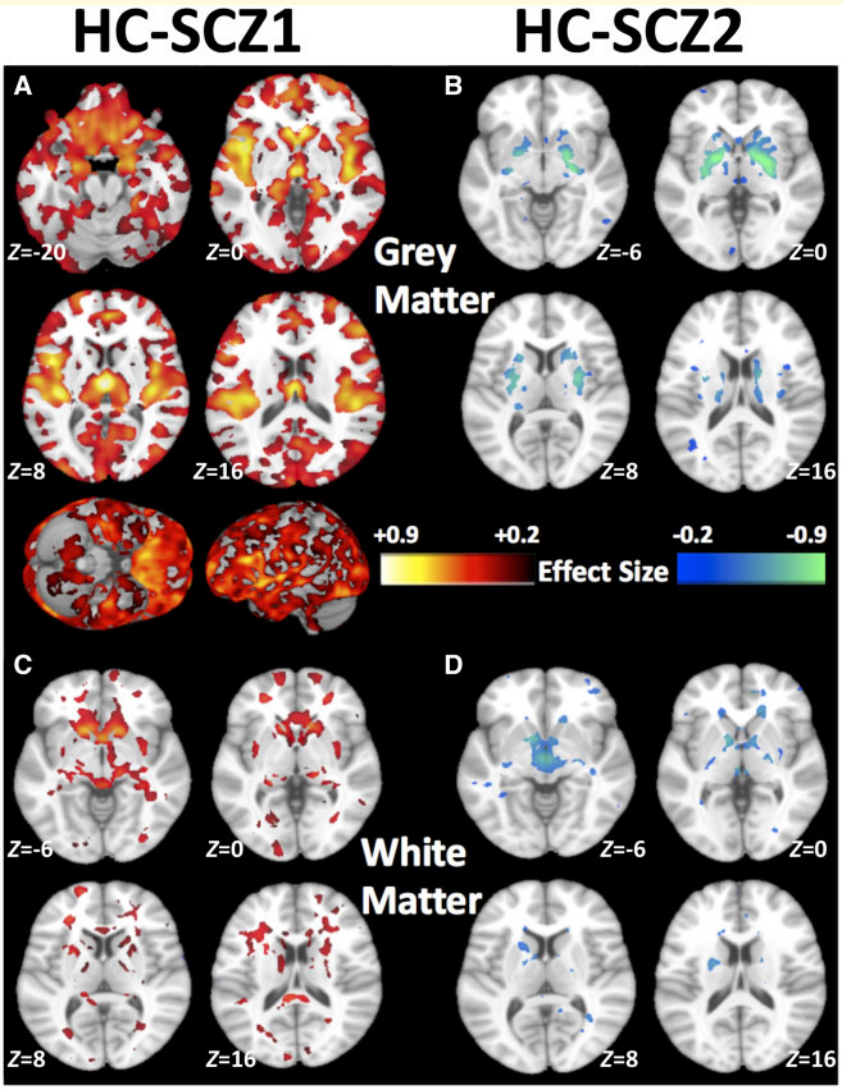

Figure 2 Patterns of grey and white matter volumes identifying the two subtypes. Compared to healthy controls (HC), (**A**) schizophrenia Subtype 1 (SCZ1) exhibits widespread patterns of smaller grey matter volumes especially in the thalamus, nucleus accumbens, medial temporal, medial prefrontal/frontal and insular cortices, (**B**) schizophrenia Subtype 2 (SCZ2) exhibits larger grey matter volumes in the basal ganglia (pallidum, putamen, and parts of caudate), (**C**) schizophrenia Subtype 1 shows smaller white matter volumes, and (**D**) schizophrenia Subtype 2 shows larger white matter volumes, especially in the internal capsule. Effect size (Cohen's *d*) maps were generated from regional volumetric maps masked by the set of regions that showed statistically significant differences ($P_{FDR} < 0.05$) in the MIDAS analysis.

differences, medication, disease chronicity, or tissue contrast. First, to ensure these findings were not influenced by differences in sample sizes (Subtype 1: $n = 192$; Subtype 2: $n = 115$), we repeated the analysis in a subset of Subtype 1 ($n = 115$) and found consistent patterns (Supplementary Fig. 11). Second, Subtype 1 abnormalities were widespread and Subtype 2 had larger basal ganglia in both males and females (Supplementary Fig. 12). Third, to assess the potential contributions of medication (Navari and Dazzan, 2009; Ansell *et al.*, 2015; Vita *et al.*, 2015), we adjusted for antipsychotic dose (chlorpromazine equivalents, CPZ). Consistent with the results shown in Fig. 2, subtype profiles were still present after controlling for chlorpromazine (Supplementary Figs 13 and 14), albeit the sample size and corresponding statistical power was substantially lower in this subsample with medication information. Fourth, we further limited the analysis to schizophrenia samples with illness duration $\leqslant$ 2 years (~1/3 of total schizophrenia samples; average illness duration 0.54 years) to attenuate the effects of disease chronicity (Supplementary Figs 15–17). Although we observed similarity between the full schizophrenia samples (Fig. 2) and the schizophrenia samples with illness duration $\leqslant$ 2 years (Supplementary Fig. 15), there were some apparent differences in the spatial distribution of the grey matter deficit, such as in insular cortex, in the early phase group. Finally, we examined the sum of grey and white matter volumes (i.e. total brain volume) to ensure the findings were not driven by image-contrast variations that

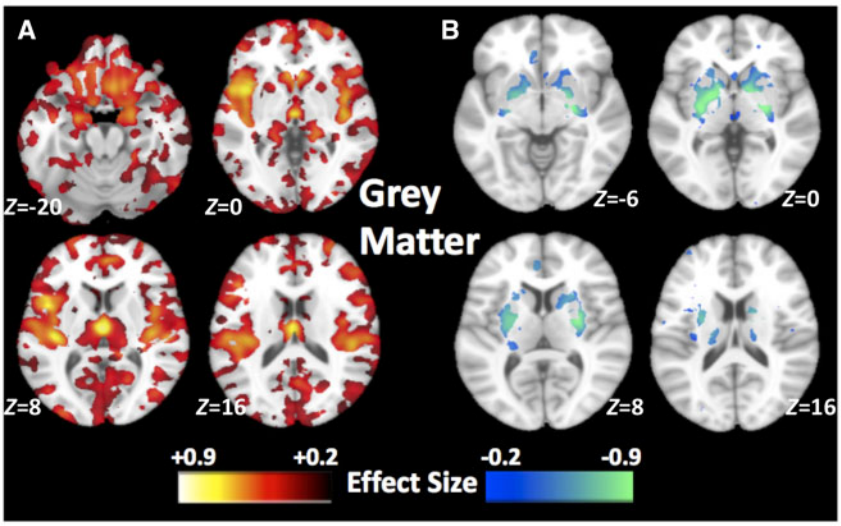

Figure 3 Reproducibility analysis. Patterns of grey matter volumes in the two subtypes using the leave-one-site-out validation: Compared to healthy control (HC), (**A**) schizophrenia Subtype 1 (SCZ1) shows widespread smaller volumes prominently in the thalamus, nucleus accumbens, medial temporal, medial prefrontal/frontal and insular cortices, and (**B**) Subtype 2 (SCZ2) shows larger volume in the basal ganglia. Effect size maps were generated from regional volumetric maps masked by the set of regions that showed statistically significant differences ($P_{FDR} < 0.05$) in the MIDAS analysis.

affect grey/white matter segmentation. This analysis yielded subtype patterns consistent with the primary analysis (Supplementary Fig. 18).

Educational attainment is lower in Subtype 1

Educational attainment was lower in Subtype 1 (chi-square = 6.389, df = 2, $P = 0.041$), but the two subtypes did not differ in age, sex, illness duration, antipsychotic dose, age of illness onset, symptom severity, or antipsychotic type (Table 2).

Grey matter volume negatively correlated with illness duration in Subtype 1

Grey matter volume was negatively correlated with illness duration in Subtype 1 ($r = -0.201$; $P = 0.016$) but not in Subtype 2 ($r = -0.045$; $P = 0.652$) (Fig. 4).

Discussion

We identified two markedly distinct neuroanatomical subtypes of schizophrenia. Subtype 1 showed a commonly reported pattern of widespread reduced grey matter relative to healthy controls (Koutsouleris *et al.*, 2008; Shenton *et al.*, 2010; Gupta *et al.*, 2015; Clementz *et al.*, 2016; Rozycki *et al.*, 2018), whereas Subtype 2 demonstrated increased volume of the basal ganglia and internal capsule against a background of normal grey and white matter. The overall findings of this study are summarized in Fig. 5.

The two subtypes were robust to permutation tests, split sample experiments, leave-one-site-out experiments, sex-specific analyses, antipsychotic-dose adjustment, and restriction to patients with less than 2 years of illness duration. Critically, standard case-control comparisons obscured the fact that average differences in schizophrenia are derived from different neuroanatomical subtypes, with grey matter decreases contributed only by approximately two-thirds of the patient population, and subcortical increases contributed only by approximately one-third of the patient population. Recent studies using normative models (Wolfers *et al.*, 2018) also suggested that such average group differences in schizophrenia disguise biological heterogeneity and objectively defining biological subtypes is a logical next step. In line with emerging recognition of neuroimaging heterogeneity (Voineskos *et al.*, 2019), our analysis revealed subtypes not otherwise detectible by (relatively crude) clinical phenotyping, but which likely have yet-to-be-discovered clinical implications. Our findings thus challenge dominant views of widespread brain volume reduction in schizophrenia, clarify previous case-control findings, and for the first time suggest a fundamental brain difference between subtypes of individuals with schizophrenia that are not sharply defined by chronicity or standard clinical measures. Below, we consider key possibilities raised by our findings in the context of the existing literature.

Table 2 Comparison between patients with schizophrenia Subtypes 1 and 2 for demographic and clinical measures

	SCZ1	SCZ2	SCZ1 versus SCZ2
n (%)	192 (62.54)	115 (37.46)	
Age, mean years (SD)	30.41 (7.26)	31.79(7.38)	*t*-stat = –1.603, df = 305, *P* = 0.109
Female, *n* (%)	68 (35.42)	40 (34.78)	χ^2 stat = 0.013, df = 1, *P* = 0.910
Duration of illness, mean years (SD), *n*	7.07 (7.41), 174	7.22 (7.42), 105	*t*-stat = –0.167, df = 277, *P* = 0.868
CPZ, mean (SD), *n*	409.78 (339.83), 125	441.35 (361.63), 87	*t*-stat = –0.439, df = 210, *P* = 0.521
Age of illness onset, mean years (SD), *n*	23.42 (6.43), 174	24.53 (7.05), 105	*t*-stat = –1.355, df = 277, *P* = 0.177
Positive symptoms, mean (SD), *n*	17.45 (7.55), 180	17.23 (6.74), 111	*t*-stat = 0.249, df = 289, *P* = 0.803
Negative symptoms, mean (SD), *n*	19.66 (8.26), 180	19.50 (9.12), 111	*t*-stat = 0.151, df = 289, *P* = 0.879
Education, *n* [ordinal scale (%)]	144 [1 (19.44), 2 (38.89), 3 (41.67)]	75 [1 (13.33), 2 (29.33), 3 (57.34)]	χ^2 stat = 6.389, df = 2, *P* = 0.041
Antipsychotic type, *n*	136	71	χ^2 stat = 6.670, df = 3, *P* = 0.083
FGAs, *n* (%)	26 (19.12)	17 (23.94)	
SGAs, *n* (%)	82 (60.29)	42 (59.19)	
FGAs + SGAs, *n* (%)	9 (6.62)	9 (12.68)	
Neither FGAs nor SGAs, *n* (%)	19 (13.97)	3 (4.23)	

FGAs = first generation antipsychotics; SCZ1 = schizophrenia Subtype 1; SCZ2 = schizophrenia Subtype 2; SGAs = second generation antipsychotics.

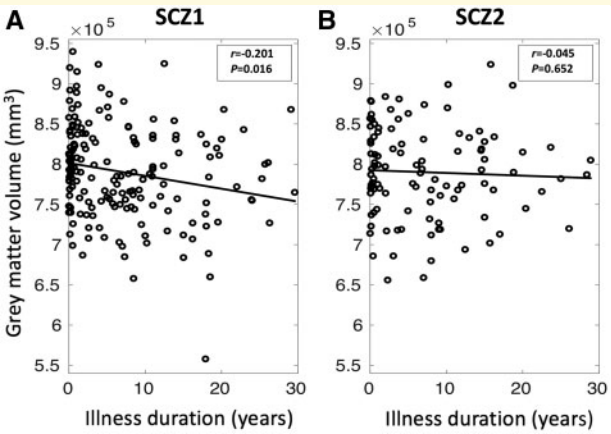

Figure 4 Associations between total grey matter volume and illness duration in the two subtypes. (**A**) Grey matter volume is correlated negatively with illness duration in schizophrenia Subtype 1 (SCZ1; r = –0.201 and P_{FDR} = 0.016), but (**B**) grey matter volume is not significantly correlated with illness duration in schizophrenia Subtype 2 (SCZ2; r = –0.045 and *P* = 0.652).

Neuroanatomical patterns and potential mechanisms

Since early pneumoencephalographic studies, a consensus has formed that individuals diagnosed with schizophrenia exhibit grey matter reductions and ventricular enlargement (Shenton *et al.*, 2010), which has been supported by recent meta- and mega-analyses (Haijma *et al.*, 2013; Gupta *et al.*, 2015). Our study clarifies that this 'average schizophrenia' pattern is only present in a percentage of the population studied (e.g. ~63% of this sample) that are contained within Subtype 1. In this subtype, the observed grey matter decrements are consistent with a mega-analysis reporting maximal volume deficits in insula (Gupta *et al.*, 2015), a multisite study revealing atrophy in medial frontal, temporo-limbic and peri-sylvian cortices (Rozycki *et al.*, 2018), and the ENIGMA and COCORO consortia showing reductions in hippocampus, thalamus and nucleus accumbens (Okada *et al.*, 2016; van Erp *et al.*, 2016). Our study also clarifies previous reports of subcortical grey matter increases (Oertel-Knöchel *et al.*, 2012; Zhang *et al.*, 2015*b*; Okada *et al.*, 2016; van Erp *et al.*, 2016) and elevated inter-individual variability in several structures including putamen (Brugger and Howes, 2017). Here, we found that increased basal ganglia volume only occurs in a proportion of individuals (~37% in this study) who show no cortical grey matter reductions. These results challenge the conventional notion that brain volume loss is a general feature of schizophrenia (Shenton *et al.*, 2010). This selective increase is notable given the high concentration of dopamine and D2/3 receptors in this region (Fusar-Poli and Meyer-Lindenberg, 2013;

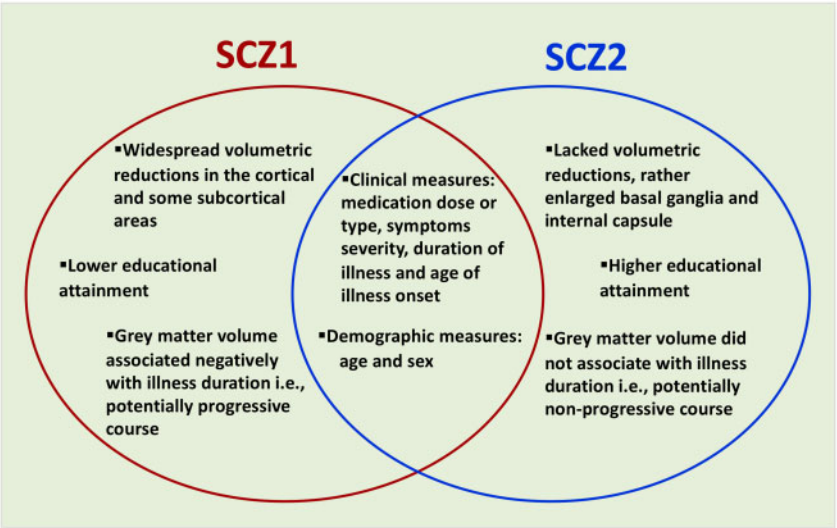

Figure 5 Summary of schizophrenia Subtypes 1 (SCZ1) and 2 (SCZ2).

Cannon, 2015) and increasing evidence in medication-naïve, clinical-risk, and genetic-risk psychosis populations indicates striatal hyperdopaminergia and larger basal ganglia (Oertel-Knöchel *et al.*, 2012; Chemerinski *et al.*, 2013; Zhang *et al.*, 2015*b*; Okada *et al.*, 2018). Schizophrenia polygenic risk and single risk alleles also associate with larger putamen in non-clinical samples (Luo *et al.*, 2019). Further, a recent study found increased putamen volume in a transdiagnostic medication-naïve sample and unaffected family members (Gong *et al.*, 2019). In combination, our findings may suggest a primary hyperdopaminergia schizophrenia subtype that has not been previously detected. In contrast to the restricted volume increase of Subtype 2, the widespread volume decreases in Subtype 1 are more consistent with mechanisms associated with early neurodevelopmental disruption, inflammation, and cortical dysfunction, where exaggerated activity of the complement-microglia system can produce synaptic over-pruning and impair interneuron migration (Howes and McCutcheon, 2017; Allswede and Cannon, 2018). Interneuron dysfunction, and aberrant cortical development more broadly, is also linked to hyperglutamatergia (Howes *et al.*, 2015) and disrupted excitatory/inhibitory balance in the cortex (Howes *et al.*, 2015; Uhlhaas and Singer, 2015). While these mechanisms could result in secondary dopaminergic disruption (Howes and Kapur, 2009), the existence of primary non-dopaminergic abnormalities could render Subtype 1 patients less responsive to current dopamine-blocking antipsychotics.

Relationship to clinical features and to prior subtypes

While neuroanatomical heterogeneity has been investigated before by determining subtypes on the basis of symptom profiles rather than brain morphology, those studies commonly revealed overlapping patterns of grey matter reductions (Koutsouleris *et al.*, 2008; Nenadic *et al.*, 2010, 2015; Voineskos *et al.*, 2013) and did not clearly distinguish between grey matter increases and decreases in different subtypes as we have done here. Our approach also overcomes the limitations of the two other neuroanatomically-driven subtyping studies (Honnorat *et al.*, 2017; Dwyer *et al.*, 2018). Those studies were limited by insufficient sample diversity and small sample size, which impeded rigorous reproducibility analyses of the clusters. Moreover, standard clustering methods used in Dwyer *et al.* (2018) are confounded by heterogeneity introduced by demographic and other disease-unrelated factors, rather than focusing on heterogeneity of disease effects. The present study sought to overcome those limitations and detected highly reproducible and distinguishable neuroanatomical subtypes. Clinically, our Subtype 1 included individuals with lower premorbid functioning (lower educational achievement) and in whom longer illness duration was associated with larger grey matter deficit. In previous comparisons of dichotomous subtypes based on clinical phenotypes (e.g. deficit versus non-deficit subtypes), negative symptom severity was associated with widespread volume deficits (Koutsouleris *et al.*, 2008; Nenadic *et al.*, 2010, 2015; Voineskos *et al.*, 2013), progressive volume loss (McKechanie *et al.*, 2016), and worse longitudinal outcomes (Gutierrez-Galve *et al.*, 2015). However, our results differ from this clinical phenotype in two important respects. First, ~63% of our sample was classified as belonging to Subtype 1, which is significantly higher than the ~15–25% prevalence expected for the deficit subtype (Kirkpatrick *et al.*, 2006). Second, we found no significant increase of negative symptoms in the Subtype 1 group whereas a prominent and persistent elevation in negative symptoms is the defining feature of the deficit syndrome (Kirkpatrick and

Galderisi, 2008). Crow proposed that his type II syndrome (broadly corresponding to deficit syndrome) and his type I syndrome (non-deficit) reflected partly independent pathological dimensions, and thus there should also be a mixed population characterized by a combination of both types (Crow, 1985). Our anatomical Subtype 1 may have captured a large spectrum of patients who have this anatomical subtype to varying degrees, and only a subset of Subtype 1 may have clinical features meeting the strict definition of deficit syndrome. The Scale for the Assessment of Negative Symptoms/Positive and Negative Syndrome Scale (SANS/PANSS) negative symptom measures available here are not selective for persistent primary negative symptoms but also capture secondary negative symptoms; future work specifically examining deficit syndrome may find it is enriched in Subtype 1. Importantly, patients included in Subtype 2, as in Subtype 1, had a diagnosis of established schizophrenia, experienced similar levels of symptoms, and were medicated at the same dose, all despite a lack of widespread brain abnormalities. Combined, these findings suggest that subtyping schizophrenia by using *a priori* diagnosis or clinical symptoms is not sufficient to identify distinct neuroanatomical subtypes. In contrast, neuroanatomically-based subtyping can point to unique biological subtypes, which largely overlap with respect to standard clinical characteristics.

Potential influence of antipsychotic medications and duration of illness

Previous cross-sectional and longitudinal studies have attributed findings of increased and decreased volumes to the effect of antipsychotic drugs (Navari and Dazzan, 2009; Lawrie *et al.*, 2011; Ansell *et al.*, 2015; Vita *et al.*, 2015). In general, antipsychotic treatment has been associated with reduced cortical and increased basal ganglia volume that appears to be stronger with first-generation ('typical') compared to second-generation ('atypical') antipsychotics (Navari and Dazzan, 2009; Ansell *et al.*, 2015; Vita *et al.*, 2015), and increases with cumulative exposure (Ho *et al.*, 2011). However, our subtypes did not differ with respect to antipsychotic dose, the neuroanatomical comparisons remained strong even after adjusting for CPZ mg eq/day, and the patterns were evident in subjects with <2 years duration of illness. There is also robust evidence that cortical reductions and basal ganglia enlargement also occur in medication-naïve populations with clinical and genetic risk (Zhang *et al.*, 2015*b*; Satterthwaite *et al.*, 2016; Gong *et al.*, 2019; Luo *et al.*, 2019). It is also possible that observed subtype differences may be influenced by differential consequences of antipsychotics such as greater treatment resistance (Dazzan, 2014) in Subtype 1 than Subtype 2; however, treatment resistance commonly affects ~30% of individuals (Mouchlianitis *et al.*, 2016) rather than ~63% reported here, and subtypes did not differ in symptom severity or antipsychotic dose which would likely be higher in treatment-resistant individuals.

Limitations and future work

Our findings suggest several exciting avenues and challenges for future research. This study was cross-sectional, and future longitudinal studies will need to address if and how these subtypes change over time and relate to change in clinical phenotype over time. Second, while our large multisite and multi-national sample is a strength, it also reduces the depth of clinical phenotyping shared across the full sample, and future studies should examine richer sets of aetiological and clinical, cognitive, and functional outcome measures. Third, despite the absence of antipsychotic effects observed here, it remains possible that subtype-specific cumulative medication effects or treatment resistance contributed to our findings, and further work is needed in unmedicated groups and in groups with precisely documented longitudinal medication data. Fourth, use of our method in much larger samples might result in a different clustering solution, and should be a focus of future work. We consider it unlikely that these two highly reproducible subtypes will not be identifiable in larger samples; more likely, other distinctions within these subtypes may be discovered, resulting in more fine-grained parsing of heterogeneity. Finally, these two reproducible anatomical subtypes also have dimensional aspects, and future work should explore how different degrees of expression of these two patterns relate to other features of the illness.

Conclusion

In summary, we uncovered two markedly distinct neuroanatomical subtypes of schizophrenia, thereby suggesting two neuroanatomical axes of this illness. Subtype 1 had a widespread pattern of lower grey matter volume relative to healthy controls, while Subtype 2 had relatively larger basal ganglia and internal capsule but normal cortical anatomy. These two subtypes were not revealed in case-control studies or clinical subtyping studies that did not directly account for the underlying neuroanatomical heterogeneity. Future research will provide a more detailed picture of these subtypes in relation to other aspects of brain structure and function, clinical features including cognitive performance, acute treatment response, longitudinal progression, and aetiology. These 'subtype fingerprints' will be traced in at-risk, subsyndromal and epidemiological samples. With additional research, these subtypes could contribute to precision clinical care that accounts for biological heterogeneity in diagnosis, prognosis, and treatment using widely used clinical brain imaging methods.

Funding

This work was supported by United States National Institutes of Health grant R01MH112070. Additional support was provided by S10OD023495, R01MH101111, R01MH113565, R01MH113550, R01MH112847, and

R01EB022573. The work was also supported by the PRONIA project as funded by the European Union 7th Framework Program grant 602152.

Competing interests

The authors report no conflicts of interest.

Supplementary material

Supplementary material is available at *Brain* online.

References

Abi-Dargham A, Horga G. The search for imaging biomarkers in psychiatric disorders. Nat Med 2016; 22: 1248–55.

Allswede DM, Cannon TD. Prenatal inflammation and risk for schizophrenia: a role for immune proteins in neurodevelopment. Dev Psychopathol 2018; 30: 1157–78.

Ansell BR, Dwyer DB, Wood SJ, Bora E, Brewer WJ, Proffitt TM, et al. Divergent effects of first-generation and second-generation antipsychotics on cortical thickness in first-episode psychosis. Psychol Med 2015; 45: 515–27.

Arlot S, Celisse A. A survey of cross-validation procedures for model selection. Stat Surv 2010; 4: 40–79.

Arnedo J, Svrakic DM, Del Val C, Romero-Zaliz R, Hernandez-Cuervo H. Molecular Genetics of Schizophrenia C, et al. Uncovering the hidden risk architecture of the schizophrenias: confirmation in three independent genome-wide association studies. Am J Psychiatry 2015; 172: 139–53.

Ben-Hur A, Elisseeff A, Guyon I. A stability based method for discovering structure in clustered data. Pac Symp Biocomput 2002; 7: 6–17.

Brugger SP, Howes OD. Heterogeneity and homogeneity of regional brain structure in schizophrenia: a meta-analysis. JAMA Psychiatry 2017; 74: 1104–11.

Cannon TD. How schizophrenia develops: cognitive and brain mechanisms underlying onset of psychosis. Trends Cogn Sci 2015; 19: 744–56.

Carpenter WT, Kirkpatrick B. The heterogeneity of the long-term course of schizophrenia. Schizophr Bull 1988; 14: 645–52.

Chemerinski E, Byne W, Kolaitis JC, Glanton CF, Canfield EL, Newmark RE, et al. Larger putamen size in antipsychotic-naive individuals with schizotypal personality disorder. Schizophr Res 2013; 143: 158–64.

Clementz BA, Sweeney JA, Hamm JP, Ivleva EI, Ethridge LE, Pearlson GD, et al. Identification of distinct psychosis biotypes using brain-based biomarkers. Am J Psychiatry 2016; 173: 373–84.

Crow TJ. The two-syndrome concept: origins and current status. Schizophr Bull 1985; 11: 471–88.

Davatzikos C, Genc A, Xu D, Resnick SM. Voxel-based morphometry using the RAVENS maps: methods and validation using simulated longitudinal atrophy. NeuroImage 2001; 14: 1361–9.

Dazzan P. Neuroimaging biomarkers to predict treatment response in schizophrenia: the end of 30 years of solitude? Dialogues Clin Neurosci 2014; 16: 491–503.

Derks EM, Allardyce J, Boks MP, Vermunt JK, Hijman R, Ophoff RA, et al. Kraepelin was right: a latent class analysis of symptom dimensions in patients and controls. Schizophr Bull 2012; 38: 495–505.

Dong A, Toledo JB, Honnorat N, Doshi J, Varol E, Sotiras A, et al. Heterogeneity of neuroanatomical patterns in prodromal Alzheimer's disease: links to cognition, progression and biomarkers. Brain 2017; 140: 735–47.

Doshi J, Erus G, Ou Y, Resnick SM, Gur RC, Gur RE, et al. MUSE: mUlti-atlas region Segmentation utilizing Ensembles of registration algorithms and parameters, and locally optimal atlas selection. NeuroImage 2016; 127: 186–95.

Du Y, Pearlson GD, Liu J, Sui J, Yu Q, He H, et al. A group ICA based framework for evaluating resting fMRI markers when disease categories are unclear: application to schizophrenia, bipolar, and schizoaffective disorders. NeuroImage 2015; 122: 272–80.

Dwyer DB, Cabral C, Kambeitz-Ilankovic L, Sanfelici R, Kambeitz J, Calhoun V, et al. Brain subtyping enhances the neuroanatomical discrimination of schizophrenia. Schizophr Bull 2018; 44: 1060–9.

Fair DA, Bathula D, Nikolas MA, Nigg JT. Distinct neuropsychological subgroups in typically developing youth inform heterogeneity in children with ADHD. Proc Natl Acad Sci U S A 2012; 109: 6769–74.

Fett AK, Viechtbauer W, Dominguez MD, Penn DL, van Os J, Krabbendam L. The relationship between neurocognition and social cognition with functional outcomes in schizophrenia: a meta-analysis. Neurosci Biobehav Rev 2011; 35: 573–88.

Fusar-Poli P, Meyer-Lindenberg A. Striatal presynaptic dopamine in schizophrenia, part II: meta-analysis of [(18)F/(11)C]-DOPA PET studies. Schizophr Bull 2013; 39: 33–42.

Gong Q, Scarpazza C, Dai J, He M, Xu X, Shi Y, et al. A transdiagnostic neuroanatomical signature of psychiatric illness. Neuropsychopharmacol 2019; 44: 869–75.

Gupta CN, Calhoun VD, Rachakonda S, Chen J, Patel V, Liu J, et al. Patterns of bray matter abnormalities in schizophrenia based on an international mega-analysis. Schizophr Bull 2015; 41: 1133–42.

Gutierrez-Galve L, Chu EM, Leeson VC, Price G, Barnes TR, Joyce EM, et al. A longitudinal study of cortical changes and their cognitive correlates in patients followed up after first-episode psychosis. Psychol Med 2015; 45: 205–16.

Haijma SV, Van Haren N, Cahn W, Koolschijn PC, Hulshoff Pol HE, Kahn RS. Brain volumes in schizophrenia: a meta-analysis in over 18 000 subjects. Schizophr Bull 2013; 39: 1129–38.

Ho BC, Andreasen NC, Ziebell S, Pierson R, Magnotta V. Long-term antipsychotic treatment and brain volume: a longitudinal study of first-episode schizophrenia. Arch Gen Psychiatry 2011; 68: 128–37.

Honnorat N, Dong A, Meisenzahl-Lechner E, Koutsouleris N, Davatzikos C. Neuroanatomical heterogeneity of schizophrenia revealed by semi-supervised machine learning methods. Schizophr Res 2017; 214: 43–50.

Howes O, McCutcheon R, Stone J. Glutamate and dopamine in schizophrenia: an update for the 21st century. J Psychopharmacol 2015; 29: 97–115.

Howes OD, Kapur S. The dopamine hypothesis of schizophrenia: version III–the final common pathway. Schizophr Bull 2009; 35: 549–62.

Howes OD, McCutcheon R. Inflammation and the neural diathesis-stress hypothesis of schizophrenia: a reconceptualization. Transl Psychiatry 2017; 7: e1024.

Hubert L, Arabie P. Comparing partitions. J Classif 1985; 2: 193–218.

Insel TR, Cuthbert BN. Brain disorders? Precisely Sci 2015; 348: 499–500.

Kirkpatrick B, Fenton WS, Carpenter WT Jr, Marder SR. The NIMH-MATRICS consensus statement on negative symptoms. Schizophr Bull 2006; 32: 214–9.

Kirkpatrick B, Galderisi S. Deficit schizophrenia: an update. World Psychiatry 2008; 7: 143–7.

Koutsouleris N, Gaser C, Jager M, Bottlender R, Frodl T, Holzinger S, et al. Structural correlates of psychopathological symptom dimensions in schizophrenia: a voxel-based morphometric study. NeuroImage 2008; 39: 1600–12.

Lange T, Roth V, Braun ML, Buhmann JM. Stability-based validation of clustering solutions. Neural Comput 2004; 16: 1299–323.

Lawrie SM, Olabi B, Hall J, McIntosh AM. Do we have any solid evidence of clinical utility about the pathophysiology of schizophrenia? World Psychiatry 2011; 10: 19–31.

Luo Q, Chen Q, Wang W, Desrivières S, Quinlan EB, Jia T, et al. Association of a schizophrenia-risk nonsynonymous variant with putamen volume in adolescents: a voxelwise and genome-wide association study. JAMA Psychiatry 2019; 76: 435–45.

McKechanie AG, Moorhead TW, Stanfield AC, Whalley HC, Johnstone EC, Lawrie SM, et al. Negative symptoms and longitudinal grey matter tissue loss in adolescents at risk of psychosis: preliminary findings from a 6-year follow-up study. Br J Psychiatry 2016; 208: 565–70.

Mouchlianitis E, McCutcheon R, Howes O. Brain imaging studies of treatment-resistant schizophrenia: a systematic review. Lancet Psychiatry 2016; 3: 451–63.

Navari S, Dazzan P. Do antipsychotic drugs affect brain structure? A systematic and critical review of MRI findings. Psychol Med 2009; 39: 1763–77.

Nenadic I, Sauer H, Gaser C. Distinct pattern of brain structural deficits in subsyndromes of schizophrenia delineated by psychopathology. NeuroImage 2010; 49: 1153–60.

Nenadic I, Yotter RA, Sauer H, Gaser C. Patterns of cortical thinning in different subgroups of schizophrenia. Br J Psychiatry 2015; 206: 479–83.

Nichols TE, Homes AP. Nonparametric permutation tests for functional neuroimaging: a primer with examples. Hum Brain Mapp 2001; 15: 1–25.

Oertel-Knöchel V, Knöchel C, Matura S, Rotarska-Jagiela A, Magerkurth J, Prvulovic D, et al. Cortical–basal ganglia imbalance in schizophrenia patients and unaffected first-degree relatives. Schizophr Res 2012; 138: 120–7.

Okada N, Fukunaga M, Yamashita F, Koshiyama D, Yamamori H, Ohi K, et al. Abnormal asymmetries in subcortical brain volume in schizophrenia. Mol Psychiatry 2016; 21: 1460–6.

Okada N, Yahata N, Koshiyama D, Morita K, Sawada K, Kanata S, et al. Abnormal asymmetries in subcortical brain volume in early adolescents with subclinical psychotic experiences. Transl Psychiatry 2018; 8: 254.

Palaniyappan L, Marques TR, Taylor H, Handley R, Mondelli V, Bonaccorso S, et al. Cortical folding defects as markers of poor treatment response in first-episode psychosis. JAMA Psychiatry 2013; 70: 1031–40.

Rozycki M, Satterthwaite TD, Koutsouleris N, Erus G, Doshi J, Wolf DH, et al. Multisite machine learning analysis provides a robust structural imaging signature of schizophrenia detectable across diverse patient populations and within individuals. Schizophr Bull 2018; 44: 1035–44.

Satterthwaite TD, Wolf DH, Calkins ME, Vandekar SN, Erus G, Ruparel K, et al. Structural brain abnormalities in youth with psychosis spectrum symptoms. JAMA Psychiatry 2016; 73: 515–24.

Satterthwaite TD, Wolf DH, Loughead J, Ruparel K, Valdez JN, Siegel SJ, et al. Association of enhanced limbic response to threat with decreased cortical facial recognition memory response with schizophrenia. Am J Psychiatry 2010; 167: 418–26.

Shenton ME, Whitford TJ, Kubicki M. Structural neuroimaging in schizophrenia: from methods to insights to treatments. Dialogues Clin Neurosci 2010; 12: 317–32.

Uhlhaas PJ, Singer W. Oscillations and neuronal dynamics in schizophrenia: the search for basic symptoms and translational opportunities. Biol Psychiatry 2015; 77: 1001–9.

van Erp TG, Hibar DP, Rasmussen JM, Glahn DC, Pearlson GD, Andreassen OA, et al. Subcortical brain volume abnormalities in 2028 individuals with schizophrenia and 2540 healthy controls via the ENIGMA consortium. Mol Psychiatry 2016; 21: 547–53.

Varol E, Sotiras A, Davatzikos C. MIDAS: regionally linear multivariate discriminative statistical mapping. NeuroImage 2018; 174: 111–26.

Varol E, Sotiras A, Davatzikos C. Alzheimer's Disease Neuroimaging I. HYDRA: revealing heterogeneity of imaging and genetic patterns through a multiple max-margin discriminative analysis framework. NeuroImage 2017; 145: 346–64.

Vita A, De Peri L, Deste G, Barlati S, Sacchetti E. The effect of antipsychotic treatment on cortical gray matter changes in schizophrenia: does the class matter? a meta-analysis and meta-regression of longitudinal magnetic resonance imaging studies. Biol Psychiatry 2015; 78: 403–12.

Voineskos AN, Foussias G, Lerch J, Felsky D, Remington G, Rajji TK, et al. Neuroimaging evidence for the deficit subtype of schizophrenia. JAMA Psychiatry 2013; 70: 472–80.

Voineskos AN, Jacobs GR, Ameis SH. Neuroimaging heterogeneity in psychosis: neurobiological underpinnings and opportunities for prognostic and therapeutic innovation. Biol Psychiatry 2019;

Wolf DH, Satterthwaite TD, Kantrowitz JJ, Katchmar N, Vandekar L, Elliott MA, et al. Amotivation in schizophrenia: integrated assessment with behavioral, clinical, and imaging measures. Schizophr Bull 2014; 40: 1328–37.

Wolfers T, Doan NT, Kaufmann T, Alnaes D, Moberget T, Agartz I, et al. Mapping the heterogeneous phenotype of schizophrenia and bipolar disorder using normative models. JAMA Psychiatry 2018; 75: 1146–55.

Zhang W, Deng W, Yao L, Xiao Y, Li F, Liu J, et al. Brain structural abnormalities in a group of never-medicated patients with long-term schizophrenia. Am J Psychiatry 2015b; 172: 995–1003.

Zhang T, Koutsouleris N, Meisenzahl E, Davatzikos C. Heterogeneity of structural brain changes in subtypes of schizophrenia revealed using magnetic resonance imaging pattern analysis. Schizophr Bull 2015a; 41: 74–84.

Zhu J, Zhuo C, Liu F, Xu L, Yu C. Neural substrates underlying delusions in schizophrenia. Sci Rep 2016; 6: 33857.

Zhuo C, Ma X, Qu H, Wang L, Jia F, Wang C. Schizophrenia patients demonstrate both inter-voxel level and intra-voxel level white matter alterations. PLoS One 2016; 11: e0162656.